

## Adaptation of a Thermorheological Lava Flow Model for Venus Conditions



### Key Points:

- We model the thermorheological properties of lava during flow emplacement under Venus conditions
- For this model, coupling atmospheric convective and radiative heat loss has a significant impact on the modeled Venus flow
- Using equivalent starting parameters, a basaltic channelized lava flow would travel ~75% further on Venus than on Earth

### Correspondence to:

I. T. W. Flynn,  
[itf2@pitt.edu](mailto:itf2@pitt.edu)

### Citation:

Flynn, I. T. W., Chevrel, M. O., & Ramsey, M. S. (2023). Adaptation of a thermorheological lava flow model for Venus conditions. *Journal of Geophysical Research: Planets*, 128, e2022JE007710. <https://doi.org/10.1029/2022JE007710>

Received 8 DEC 2022  
Accepted 31 MAY 2023

### Author Contributions:

**Conceptualization:** Ian. T. W. Flynn, Michael. S. Ramsey

**Formal analysis:** Ian. T. W. Flynn, Magdalena. O. Chevrel

**Funding acquisition:** Michael. S. Ramsey

**Investigation:** Ian. T. W. Flynn

**Methodology:** Ian. T. W. Flynn, Magdalena. O. Chevrel

**Project Administration:** Michael. S. Ramsey

**Resources:** Michael. S. Ramsey

**Supervision:** Michael. S. Ramsey

**Visualization:** Ian. T. W. Flynn

**Writing – original draft:** Ian. T. W. Flynn

**Writing – review & editing:** Ian. T. W. Flynn, Magdalena. O. Chevrel, Michael. S. Ramsey

Ian. T. W. Flynn<sup>1</sup> , Magdalena. O. Chevrel<sup>2,3,4</sup> , and Michael. S. Ramsey<sup>1</sup> 

<sup>1</sup>Department of Geology and Environmental Science, University of Pittsburgh, Pittsburgh, PA, USA, <sup>2</sup>Laboratoire Magmas et Volcans (LMV), CNRS, IRD, OPGC, Université Clermont Auvergne, Clermont-Ferrand, France, <sup>3</sup>Observatoire Volcanologique du Piton de la Fournaise, Institut de Physique du Globe de Paris, La Plaine des Cafres, France, <sup>4</sup>Institut de Physique du Globe de Paris, CNRS, Université Paris Cité, Paris, France

**Abstract** Active volcanism was (and potentially still is) an important process that shapes the Venus surface and its detection is a primary goal for the planned VERITAS and EnVision missions. Therefore, understanding lava flow emplacement and timing on Venus is important. We adapt the terrestrial PyFLOWGO thermorheological model to Venus conditions to assess the effects on channelized lava flow propagation. We first initiate the model with terrestrial basaltic parameters and progressively adapt it to Venusian conditions in five steps: (a) gravity, (b) ambient atmospheric temperature, (c) specific heat capacity and wind speed, (d) atmospheric density, and (e) coupled convective and radiative heat flux. Compared to Earth, the slightly lower gravity on Venus resulted in a lower flow velocity, a higher crust coverage, and a very minor increase in flow length (0.1%). Increasing the ambient atmospheric temperature reduced heat loss and produced a (77%) longer flow; whereas next accounting for the atmospheric specific heat capacity and wind speed increased the flow length slightly more (81%). However, increasing the atmospheric density resulted in a shorter lava flow (13%) due to more efficient cooling. Finally, accounting for coupled convective and radiative heat loss due to the strong CO<sub>2</sub> infrared absorption resulted in an increase of the flow length (~75%). Although the model applies only to channelized, cooling-limited flows, these results reveal that for the same effective effusion rate and topography, a Venusian lava flow travels a longer distance than the equivalent flow on Earth and its cooling should be detectable by future orbital instruments.

**Plain Language Summary** Lava flow length and velocity is partially controlled by the environmental conditions of a planet (e.g., gravity, atmospheric temperature, and density). Observations reveal that Venus volcanism is an important process that shaped its surface. However, the extreme surface environment influences the emplacement of these lava flows differently than on Earth. In this study, we quantify the impact of the Venusian planetary and environmental conditions on lava flow advance using the PyFLOWGO model. Although this model is one-dimensional and applies only to channelized, cooling-limited flows, it is exceedingly adaptable, and by far is the most cited model in the literature. Here, we adapt an Earth lava flow to Venus conditions in five steps: (a) gravity, (b) atmospheric temperature, (c) atmospheric specific heat capacity and wind speed, (d) atmospheric density, and (e) coupling atmospheric convective and radiative heat flux. Compared to Earth conditions, the lava flow is most affected by the heat flux difference caused by the CO<sub>2</sub>-rich Venusian atmosphere, which results in a 75% longer flow than the same flow on Earth due to the decrease in heat loss to the atmosphere. Results for a 100 km Venusian lava flow indicate that it would be observable by the upcoming missions.

## 1. Introduction

Past studies highlight similarities between the volcanic features of Earth and Venus and commonly identify Venus as an important location to study planetary volcanism (Head & Wilson, 1986; Head et al., 1992; Ivanov & Head, 2013). These studies identified shield volcanoes, lava flows, variable lava textures and possible exposed dikes (e.g., Head et al., 1992; Ivanov & Head, 2013; Mouginis-Mark, 2016). More detailed investigations of the volcanic regions on Venus (i.e., Mylitta Fluctus and Astkikh Planum) identified complex flow morphologies such as channelized lava flows with well-defined levees (Byrnes & Crown, 2002; MacLellan et al., 2021; Roberts et al., 1992). These channelized, leveed flows are an important subset to understand because they typically form earlier in an eruption when the effusion rate is higher. They are also indicative of specific emplacement conditions other than effusion rate, such as higher lava velocities, and/or steeper topographic slopes (Gregg, 2017; Rowland et al., 2005).

© 2023. The Authors.

This is an open access article under the terms of the [Creative Commons Attribution-NonCommercial-NoDerivs License](https://creativecommons.org/licenses/by-nc-nd/4.0/), which permits use and distribution in any medium, provided the original work is properly cited, the use is non-commercial and no modifications or adaptations are made.

The data returned by the Magellan mission launched in 1989 and the Venus Express Mission launched in 2005 have sparked debate around the potential for recent and possibly ongoing volcanic activity (D’Incecco et al., 2017, 2021; Filiberto et al., 2020; Herrick & Hensley, 2023; Mueller et al., 2017; Smrekar et al., 2010). Byrne and Krishnamoorthy (2021) proposed that the upcoming missions to Venus might observe active volcanism. More recent work by Herrick and Hensley (2023) claims to identify new activity after reexamining Magellan data. Progress in the study of Venusian volcanology relies heavily on the use of synthetic aperture radar (SAR) data because the opaque atmosphere hinders most other wavelength regions. Current information of the surface features is therefore dependent on the SAR image resolution. Any investigation that requires moderate to high resolution images of the surface (e.g., volcanic mapping of fine scale details) is limited to 100–200 m/pixel SAR images and 10–20 km (horizontal) and 50–100 m (vertical) resolution topographic data (Ford & Pettengill, 1992; Saunders et al., 1992). Some regions of the planet have been imaged at a higher resolution SAR data (i.e., 75 m/pixel) and topography (1–2 km/pixel horizontal) (Herrick et al., 2012); however, this spatial resolution is still insufficient to identify more detailed lava flow morphology.

These limitations result in higher measurement uncertainties (i.e., length, width, and thickness) that are required for flow modeling, which in turn calculates the emplacement dynamics and rheological parameters (i.e., viscosity and yield strength) (e.g., Baloga & Glaze, 2008; Peters et al., 2021). Many of these models assume that lava flow emplacement is controlled by a cooling-limited rheology that dictates flow stoppage when the viscosity becomes too high due to cooling and crystallization (Pinkerton & Wilson, 1994). Well-known equations developed for terrestrial lava flows have been applied extensively to other terrestrial bodies to determine emplacement conditions and properties, including flow viscosity, yield strength, and effusion rate (e.g., Daneš, 1972; Hiesinger et al., 2007; Hulme, 1974, 1976; Pieri & Baloga, 1986; Vaucher et al., 2009). Other more advanced models that account for the environmental conditions and complex flow processes have also been developed and adapted to investigate planetary lava flows (e.g., Baloga & Glaze, 2008; Flynn et al., 2022; Rowland et al., 2004).

In this study, we adapt the FLOWGO model (Harris & Rowland, 2001) to Venus in order to examine how the emplacement of a channelized basaltic lava flow would differ from the same flow emplaced on Earth. Our goal is to determine an average emplacement time and cooling rate of these flows to provide a baseline estimate for the planned future missions. FLOWGO is a robust, easily adapted, and well-tested thermorheological model with a long history of Earth (e.g., Harris & Rowland, 2001; Harris et al., 2022; Ramsey et al., 2019; Rhéty et al., 2017; Rowland et al., 2005; Wantim et al., 2013; Wright et al., 2008) and Mars applications (e.g., Flynn et al., 2022; Rowland et al., 2002, 2004). This one-dimensional model computes the thermal budget of a control volume of lava in a channel and tracks the resulting cooling, viscosity, and velocity down a slope for a given constant effusion rate. The thermal budget is calculated based on three main heat loss fluxes: radiation of the hot surface, forced atmospheric convection at the contact between flow surface and atmosphere, and conduction through the basal layer, in addition to the heat gain through crystallization. The model assumes a constant channel depth and variable width to accommodate for the constant effusion rate and ensure volume conservation downflow. The flow regime is considered laminar flow and controlled by Bingham rheology. Although the model is constrained to open-channel, cooling-limited lava flows, it nonetheless serves an important role to track the evolution of lava flow dynamics with well-validated results for this type of lava flow.

Observations of Venusian flow fields have identified multiple locations (e.g., Derceto Plateau, Turgmam Fluctus, Mylitta Fluctus) with distinct channels and cooling-limited flow emplacement features (Byrnes & Crown, 2002), making FLOWGO appropriate for modeling this subset of Venusian lava flows. Here, we adapt the model to Venusian conditions, changing the planetary and environmental parameters to track the incremental changes that each produces. The results give insight into the emplacement dynamics (including maximum run out distances, velocity, crust cover, heat flux, and timing) of a flow that potentially could be emplaced during data acquisition from the suite of instruments on the upcoming missions to Venus.

## 2. Modeling Approach

To quantify the effects of a planetary environment on the emplacement of a channelized lava flow, we adopt a similar methodology as Rowland et al. (2004), who used the lava parameters of a well-known Hawaiian lava flow as the input into FLOWGO, which was adapted for Mars conditions. We opted to use the lava flow produced by Cone II (Figure 1) during the 1975 Great Tolbachik Fissure Eruption (GTFE) (Fedotov et al., 1991). This flow was initially selected because the rheological parameters were previously calibrated using FLOWGO (Table 1)

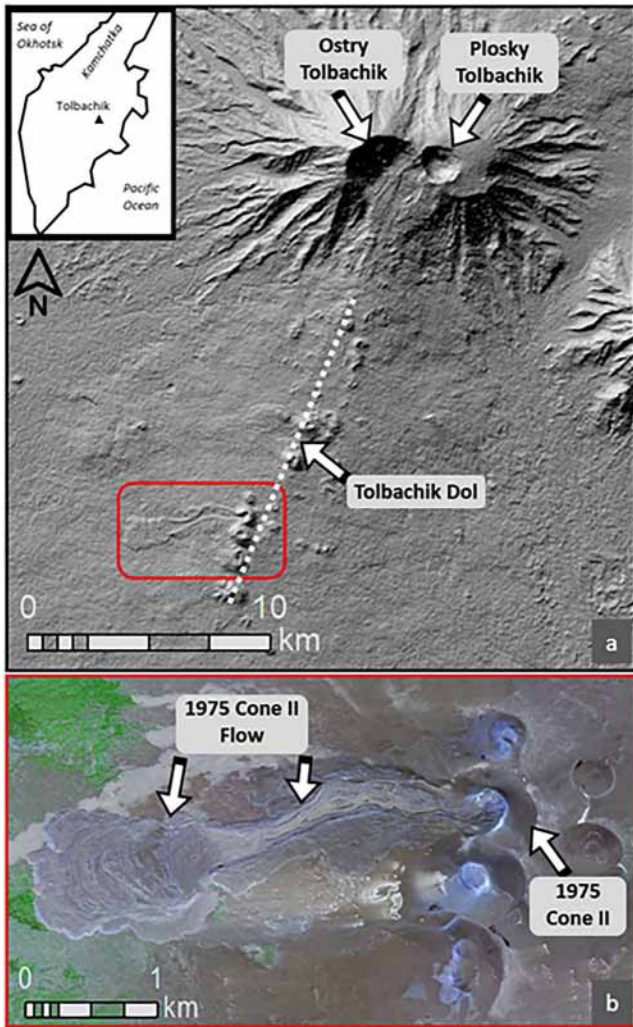


**Figure 1.** Location of the Cone II lava flow emplaced during the Great Tolbachik Fissure Eruption in 1975. (a) Tolbachik volcanic complex located on the Kamchatka peninsula, Russia. The base image is the hill-shaded global DEM v3 from Advanced Spaceborne Thermal Emission and Reflection Radiometer. The Tolbachik volcanic complex is comprised of two main edifices: Ostry and Plosky Tolbachik and to the south is the Tolbachik Dol (“valley”), an north-northeast alignment of cinder cones indicated by the white dotted line. The red box indicates the Cone II channelized flow shown in (b). (b) High resolution image of the Cone II lava flow used as an analog for this study. False color image from the Planets RapidEye Sensor (~5 m/pixel, visible), acquired on 18 June 2014.

(Ramsey et al., 2019). Moreover, several other factors lead to its use as an analog for this study. The composition of the Cone II flow is similar to that determined on Venus from the Venera and Vega series landers as basalt (i.e., tholeiitic and alkaline) (Ashley & Ramsey, 2019; Basilevsky & Head, 2003; Nikolaeva & Ariskin, 1999). Additionally, the major element composition (e.g., MgO and Al<sub>2</sub>O<sub>3</sub>) for the GTFE fall within the same range determined by the Venera and Vega landers (Churikova et al., 2015; Filiberto, 2014). Investigation of Venusian flows morphology also supports a basaltic composition (Gregg & Sakimoto, 1996; Wroblewski et al., 2019).

The Tolbachik volcanic complex is located on the Kamchatka Peninsula, Russia and is comprised of two volcanoes, Ostry Tolbachik and Plosky Tolbachik (Figure 1). In 1975, a large eruption produced an north-northeast alignment of cinder cones, associated lava flows, and ash fall referred to as Tolbachik Dol (Fedotov et al., 1991). Between 6 July and 10 September 1975, the largest cone (Cone II) produced a ~5 km long basaltic lava flow with well-developed levees ~30 m above the local topography (Figure 1) (Ramsey et al., 2019).

To adapt the model to Venusian conditions, a five-step protocol was applied. Step one decreases the gravity from 9.81 to 8.87 m/s<sup>2</sup> and is referred to here as the “Small-Earth” case. Step two increases the ambient atmospheric temperature from 273 to 740 K (Basilevsky & Head, 2003), which is referred to as the “Hot-Small-Earth” case. For step three, the atmospheric specific heat capacity is changed from 1,099 to 1,181 J/kg K and the wind speed decreased from 5 to 1 m/s (Basilevsky & Head, 2003; Lebonnois et al., 2010), both referred to as the “Venus-light” case. The fourth step, defined as the “Venus-Heavy” case, increases the atmospheric density from 0.4412 to 67 kg/m<sup>3</sup> (Basilevsky & Head, 2003). Finally, the fifth step incorporates the atmospheric heat flux model proposed in Snyder (2002), the “Simulated-Venus” case. Each of these steps is progressive, building upon the prior changes. Under the “Simulated-Venus” conditions, we also perform tests to find the effusion rate that would reproduce a 100 km long Venusian lava flow.

To limit the number of model variables assessed, two assumptions are also made. (a) All initial cases use an effective effusion rate of 700 m<sup>3</sup>/s, which is the value determined by Ramsey et al. (2019) to reproduce the Cone II lava flow length. (b) All model runs are conducted over a constant 1° slope, which removes the impact of slope-change on the results and is consistent with larger-scale topography observed across Venus (Byrnes & Crown, 2002; Flynn et al., 2021; Mouginiis-Mark, 2016; Roberts et al., 1992). All modeling is conducted using the PyFLOWGO model (<https://github.com/pyflowgo/pyflowgo>), which is the Python-coded version of FLOWGO that allows high flexibility for changing parameters (Chevrel et al., 2018).

### 2.1. Effects of Venusian Gravity (“Small-Earth”)

Decreasing the gravity has a direct influence on the modeled mean velocity ( $V_{\text{mean}}$ ) of lava traveling down the channel. PyFLOWGO calculates mean velocity using a variation of Jeffreys equation (Equation 1):

$$V_{\text{mean}} = \left[ \frac{\rho_{\text{bulk}} g d^2 \sin \theta}{n \eta_{\text{bulk}}} \right] \left[ 1 - \frac{3}{2} \frac{\tau_0}{\tau_b} + \frac{1}{2} \left( \frac{\tau_0}{\tau_b} \right)^3 \right] \quad (1)$$

where  $n$  is the channel shape factor, obtained via  $3(1 + d/w)^2$  (Wilson & Parfitt, 1993),  $\theta$  is the underlying slope in radians,  $g$  (m/s<sup>2</sup>) is the gravitational acceleration,  $\rho_{\text{bulk}}$  (kg/m<sup>3</sup>) is the bulk lava density,  $\eta_{\text{bulk}}$  (Pa s) is the bulk viscosity of the lava, and  $\tau_0$  (Pa) and  $\tau_b$  (Pa) are the lava yield strength and basal shear stress, respectively.

**Table 1**  
All PyFLOWGO Input Models and Parameters Used for the Adaptation of the Great Tolbachik Fissure Eruption (Ramsey et al., 2019) to Venusian Environmental and Planetary Conditions

Models	Selection: Earth	Selection: Venus	References
Crystallization rate	Basic	Basic	Harris and Rowland (2001) and Chevrel et al. (2018)
Melt viscosity	vft	vft	Giordano et al. (2008)
Relative viscosity	er	er	Einstein-Roscoe model from Chevrel et al. (2018)
Yield strength	Ryerson	Ryerson	Ryerson et al. (1988)
Crust temperature	Constant	Constant	Harris and Rowland (2001) and Chevrel et al. (2018)
Effective crust cover	Basic	Basic	Harris and Rowland (2001) and Chevrel et al. (2018)
Vesicle fraction	Constant	Constant	Harris and Rowland (2001) and Chevrel et al. (2018)
Heat budget modules	Selection		References
Radiation	Yes	Yes	Harris and Rowland (2001) and Ramsey et al. (2019)
Conduction	Yes	Yes	Harris and Rowland (2001)
Convection	Yes	Yes	Harris and Rowland (2001)
Rain	No	No	Harris and Rowland (2001)
Viscous heating	No	No	Harris and Rowland (2001)
Initial input parameters	Value		References
Step size	10 m	10 m	Harris and Rowland (2001) and Chevrel et al. (2018)
Effusion rate <sup>a</sup>	700 m <sup>3</sup> s <sup>-1</sup>	700 m <sup>3</sup> s <sup>-1</sup>	Ramsey et al. (2019)
Width	70 m	70 m	Ramsey et al. (2019)
Depth	8.7 m	8.7 m	Ramsey et al. (2019)
Gravity <sup>a</sup>	9.81 ms <sup>-2</sup>	8.87 ms <sup>-2</sup>	Ramsey et al. (2019)
Eruption temperature	1325 K	1325 K	Fedotov et al. (1991)
Crystal fraction	0.25	0.25	Ramsey et al. (2019)
DRE density	2,630 kg m <sup>3</sup>	2,630 kg m <sup>3</sup>	Ramsey et al. (2019)
Vesicle fraction	0.06	0.06	Ramsey et al. (2019)
Stefan-Boltzmann constant	5.60E-08	5.60E-08	Ramsey et al. (2019)
Emissivity crust	0.95	0.95	Lee and Ramsey (2016)
Emissivity uncrusted	0.6	0.6	Lee and Ramsey (2016)
Basal temperature <sup>a</sup>	773.15 K	773.15–1173 K	Harris and Rowland (2001) and Chevrel et al. (2018)
Distance from core to base	19%	19%	Harris and Rowland (2001) and Chevrel et al. (2018)
Wind speed <sup>b</sup>	5 ms <sup>-1</sup>	1 ms <sup>-1</sup>	Earth: Harris and Rowland (2001) and Chevrel et al. (2018) Venus: Basilevsky and Head (2003)
Air Ch	0.0036	0.0036	Harris and Rowland (2001) and Chevrel et al. (2018)

**Table 1**  
*Continued*

Initial input parameters	Value	References
Air temperature <sup>a</sup>	273.15 K	<i>Earth</i> : Harris and Rowland (2001) and Chevrel et al. (2018)
Air density <sup>a</sup>	0.4412 kg m <sup>-3</sup>	<i>Venus</i> : Basilevsky and Head (2003)
Air specific heat capacity <sup>a</sup>	1,099 J kg <sup>-1</sup> K <sup>-1</sup>	<i>Earth</i> : Harris and Rowland (2001) and Chevrel et al. (2018)
Buffer	140°C	<i>Venus</i> : Basilevsky and Head (2003)
Crust cover fraction	0.9	<i>Earth</i> : Harris and Rowland (2001) and Chevrel et al. (2018)
Velocity dependency of crust	-0.16	<i>Venus</i> : Lebonnois et al. (2010)
Crust temperature	773.15 K	Harris and Rowland (2001)
a vft	-4.55 Pa s	Ramsey et al. (2019)
b vft	6,887.303 J mol <sup>-1</sup>	Ramsey et al. (2019)
b vft	527.44 K	Belousov et al. (2015)
Crystal growth	0.37	Volynets et al. (2015)
Solid temperature	1,253.15 K	Volynets et al. (2015)
Latent heat of crystallization	350,000 K kg <sup>-1</sup>	Volynets et al. (2015)
		Ramsey et al. (2019)
		Ramsey et al. (2019)
		Harris and Rowland (2001) and Chevrel et al. (2018)

*Note.* For a full description of abbreviations see Chevrel et al. (2018).  
<sup>a</sup>Indicates values that vary during the study.

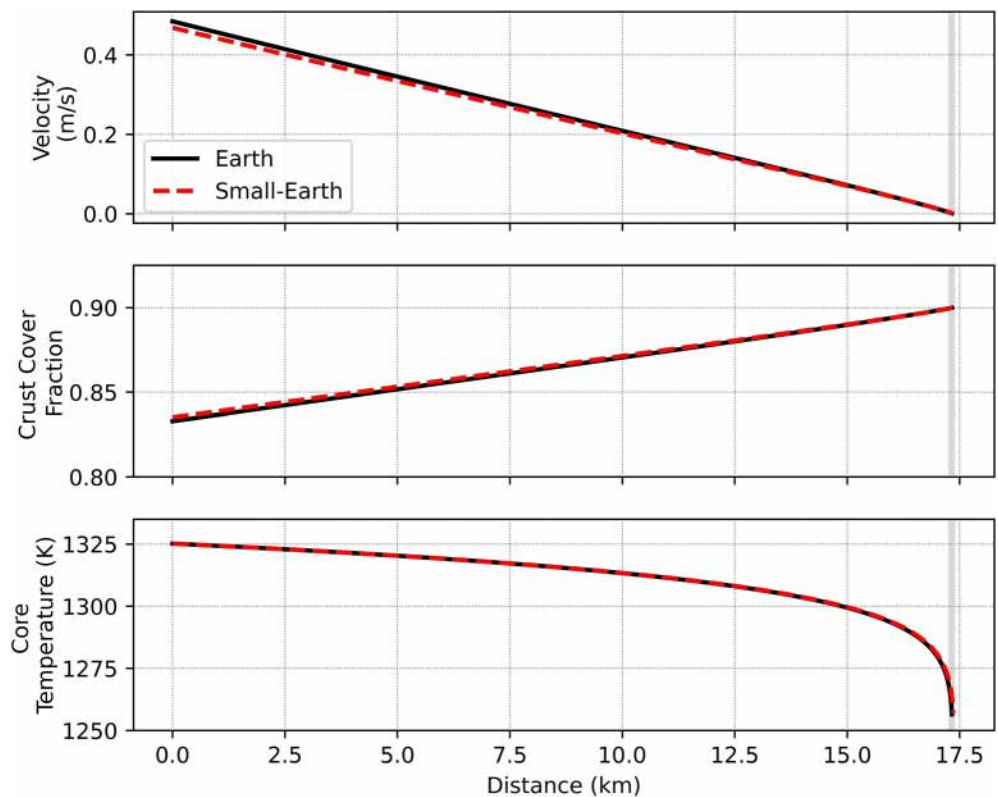


**Figure 2.** Evolution in modeled channel length with distance for the mean flow velocity, crust cover fraction, and the core temperature (from top to bottom) for the “Earth” and “Small-Earth” cases. The gray region indicates the stopping range between the two cases.

The effect of reducing the gravity from 9.81 to 8.87 m/s<sup>2</sup> and keeping all other parameters the same results in a slight increase in flow length. The baseline “Earth” case traveled a distance of 17.33 km over the constant slope, whereas the “Small-Earth” case traveled 17.36 km, a 0.1% increase. The average mean lava velocity in the channel was 0.23 m/s compared to 0.24 m/s for “Earth” (Figure 2). The slightly lower velocity for the “Small-Earth” case results in an average of 0.1% more insulating crust to form on the flow surface, which lowers the radiative heat loss allowing the flow to travel farther. This result is counter to those presented in Rowland et al. (2004) where adapting FLOWGO to the Martian environment. That study found that a decrease in gravity results in a shorter flow length but emplaced over a longer time period. We attribute the difference in results to model improvements made regarding how changes in rheology and heat flux are calculated (Chevrel et al., 2018; Ramsey et al., 2019; Thompson & Ramsey, 2021), rather than gravity. Based on this initial step and all other factors being equal, a Venusian lava flow would have a higher crust cover percent than an equivalent terrestrial flow at the same point in its emplacement.

## 2.2. Effects of Ambient Atmosphere (“Hot-Small-Earth”)

Next, the ambient atmospheric temperature was increased from 273.15 to 740 K in the model; however, all the other atmospheric variables (e.g., density, composition, wind speed) were left the same as those on Earth. This is referred to as the “Hot-Small-Earth” case. An atmospheric temperature of 740 K for the Venusian ambient atmospheric temperature is based on reported values from the prior landers; however, the surface temperature does vary across the planet with elevation and latitude, as it does on Earth (Basilevsky & Head, 2003; Pollack et al., 1980). We first test the effect of a high atmospheric temperature at 740 K and then the effect of atmospheric temperature variation. Because a higher atmospheric temperature results in a warmer surface temperature, we also test the effects of a warmer basal layer.

### 2.2.1. Atmospheric Temperature

The difference between the “Earth” and “Hot-Small-Earth” cases is notable with a 22 km (~77%) modeled flow length increase (Figure 3). Other differences between the two cases are a decrease in heat loss to the surrounding

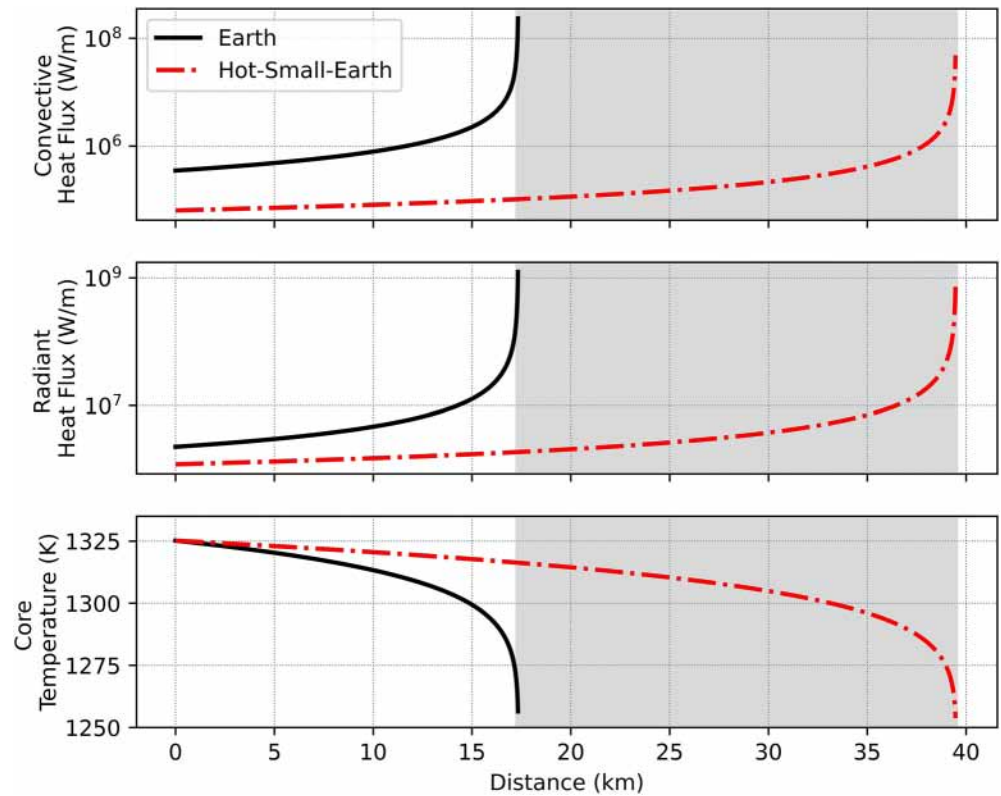


**Figure 3.** Variation in modeled channel length with distance from the vent for convective heat flux, radiant heat flux, and core temperature (from top to bottom) for the “Earth” and “Hot-Small-Earth” cases. The gray region indicates the stopping range between the two cases.

atmosphere and hence, a flow core that remains hotter longer. At a given distance, the “Hot-Small-Earth” lava flow lost less heat through radiation and atmospheric convection than the “Earth” case. An increase of flow length due to hot ambient atmosphere is consistent with the previous studies for Venus (e.g., Head & Wilson, 1986). The higher flow core temperature results in a lower rate of increase in both viscosity and yield strength at a given distance from the vent, thus allowing the flow to travel a longer distance (Figure 4).

The ambient atmospheric temperature ( $T_{\text{atmo}}$ ) is a parameter included in the equations used to determine the amount of heat lost through radiation and forced atmospheric convection. Heat loss due to radiation (Equation 2) from the lava surface to the atmosphere is expressed as follows:

$$Q_{\text{rad}} = \sigma \epsilon_{\text{eff}} T_{\text{eff}}^4 w \quad (2)$$

where  $\sigma$  (W/m<sup>2</sup>/K<sup>4</sup>) is the Stefan-Boltzmann constant,  $\epsilon_{\text{eff}}$  is the effective emissivity of the lava,  $T_{\text{eff}}$  (K) is the effective radiation temperature and  $w$  is the channel width (m). Effective emissivity is a recent addition to PyFLOWGO (Ramsey et al., 2019; Thompson & Ramsey, 2021). Here we use the model presented in Thompson and Ramsey (2021) that computes the effective emissivity based on a linear relationship with the effective radiation temperature of the lava (Pieri & Baloga, 1986).

Atmospheric temperature directly influences the flow’s effective radiation temperature ( $T_{\text{eff}}$ ) (Equation 3), which is calculated using a two-component model for the lava surface, a cooler crust surface and an un-crustified hotter lava surface (Crisp & Baloga, 1990; Pieri & Baloga, 1986; Pieri et al., 1990).

$$T_{\text{eff}} = [f_{\text{crust}} (T_{\text{crust}}^4 - T_{\text{atmo}}^4) + (1 - f_{\text{crust}}) (T_{\text{hot}}^4 - T_{\text{atmo}}^4)]^{0.25} \quad (3)$$

For Equation 3,  $T_{\text{atmo}}$  is the temperature of the ambient atmosphere,  $f_{\text{crust}}$  is the fraction of crusted lava,  $T_{\text{crust}}$  is the crust temperature, and  $T_{\text{hot}}$  is the hot component of the exposed lava surface. The various model options available to calculate  $f_{\text{crust}}$ ,  $T_{\text{crust}}$ , and  $T_{\text{hot}}$  can be found in detail in Chevrel et al. (2018). For this study, the model choices are shown in Table 1.

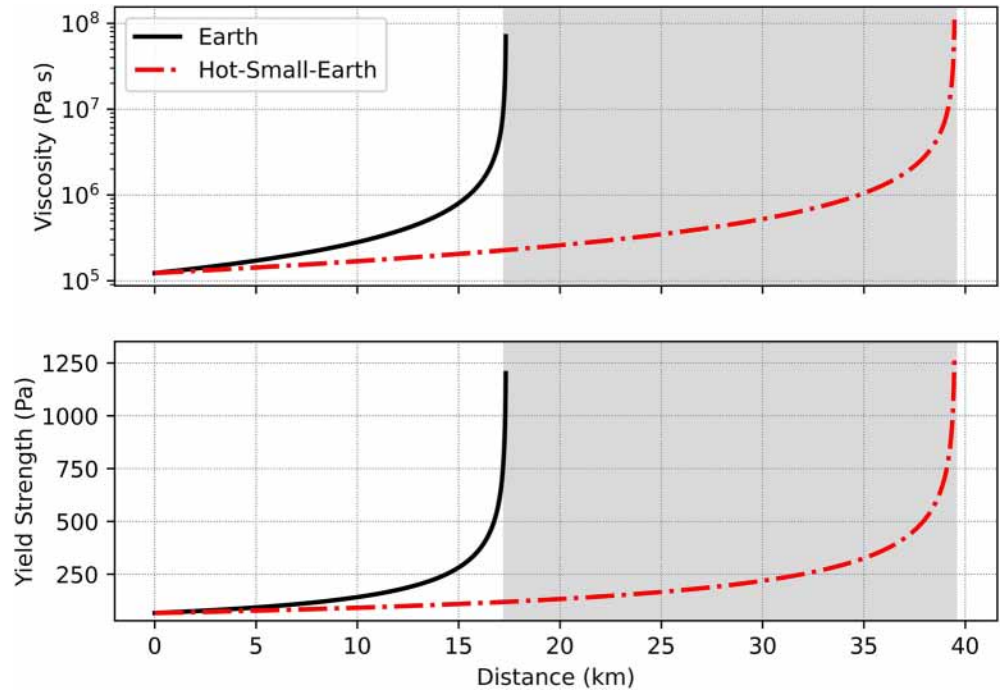


**Figure 4.** Variation in modeled channel length with distance from the vent for viscosity and yield strength for the “Earth” and “Hot-Small-Earth” cases. The gray region indicates the stopping range between the two cases.

Ambient atmospheric temperature also directly affects heat loss due to forced atmospheric convection. In PyFLOWGO, heat loss from the lava surface due to forced convection of the atmosphere is calculated using (Equation 4):

$$Q_{\text{conv}} = h_{\text{conv}}(T_{\text{conv}} - T_{\text{atmo}})w \quad (4)$$

where  $h_{\text{conv}}$  is the convective heat transfer ( $\text{W}/\text{m}^2\text{K}$ ) and  $T_{\text{conv}}$  (K) is the characteristic surface temperature. Convective heat transfer is directly linked to atmospheric conditions and is defined as (Equation 5):

$$h_{\text{conv}} = UC_H \rho_{\text{atmo}} C_{\rho_{\text{atmo}}} \quad (5)$$

where  $U$  is the wind speed (m/s),  $C_H$  the wind friction factor as defined by Greeley and Iversen (1987),  $\rho_{\text{atmo}}$  ( $\text{kg}/\text{m}^3$ ) is atmospheric density and  $C_{\rho_{\text{atmo}}}$  the atmospheric heat capacity ( $\text{J}/\text{kg K}$ ). Characteristic lava surface temperature is then defined as (Equation 6).

$$T_{\text{conv}} = [f_{\text{crust}} T_{\text{crust}}^{1.33} + (1 - f_{\text{crust}})(T_{\text{hot}}^{1.33})]^{0.75} \quad (6)$$

Between the “Earth” and “Hot-Small-Earth” cases, there is  $\sim 1.9 \times 10^6 \text{ W}/\text{m}$  and  $\sim 9.5 \times 10^6 \text{ W}/\text{m}$  less heat loss per model step due to the atmospheric convective and radiative heat flux, respectively. This comparison is useful to highlight the heat loss processes on a planetary body with a high ambient atmospheric temperature and how it influences the rheology and flow length (i.e., volcanic exoplanets deemed “lava worlds”).

### 2.2.2. Atmospheric Temperature Variations

Atmospheric temperatures across the Venusian surface vary from  $\sim 755$  to  $\sim 650 \text{ K}$  at the highest elevation on Venus (Maxwell Montes) (Basilevsky & Head, 2003). To assess how this surface variation impacts the emplacement of a channelized lava flow, the “Hot-Small-Earth” case was rerun multiple times using atmospheric temperature increments from 650 to 760 K (Figure 5). There is a positive correlation that occurs between an increase in atmospheric temperature and channel length.

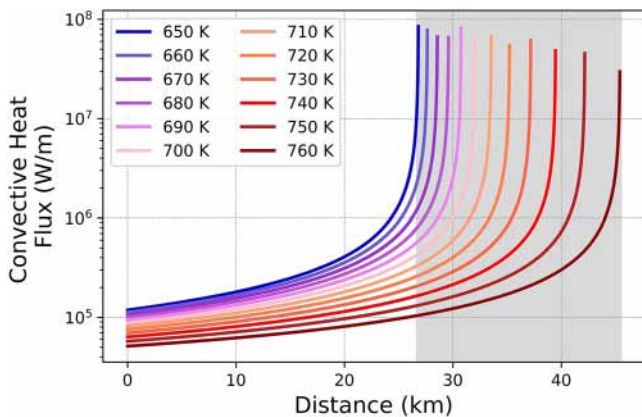


**Figure 5.** Differences in modeled channel length with distance from the vent versus convective heat flux for a range of atmospheric temperatures expected on the Venus surface. The gray region indicates the stopping range for all modeled temperatures.



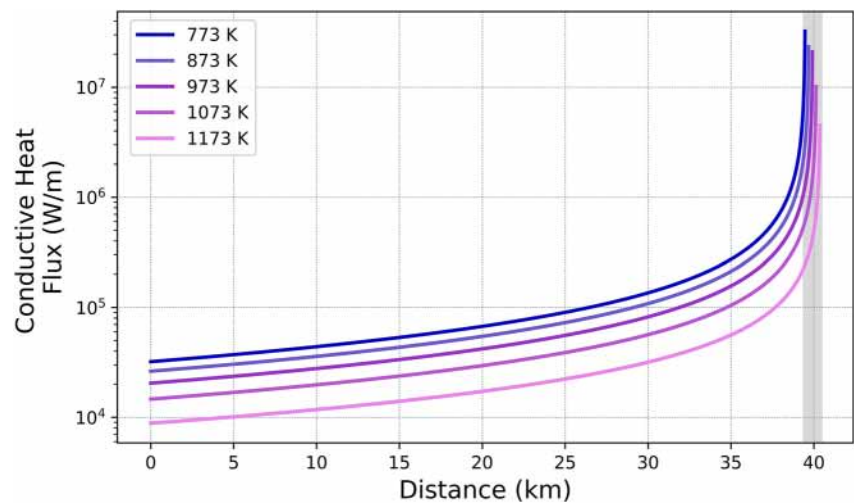


**Figure 6.** Differences in modeled channel length with distance from the vent versus conductive heat flux for a range of basal temperatures plausible for the Venusian surface. The gray region indicates the stopping range for all modeled temperatures.

For every 10 K increase in atmospheric temperature the channelized lava flow lengthened by  $\sim 1.6$  km on average, with a greater increase in length occurring at the higher ambient atmospheric temperatures (Figure 5). At an atmospheric temperature of 650 K, the flow's channel length is 26.8 km, which increases to 45.4 km at 760 K. The increase in channel length is predominantly due to the decrease in atmospheric convective heat loss (Figure 5), and the results are similar to trends in previous modeling (e.g., Zimbelman et al., 2000). For the remainder of the work, an atmospheric temperature of 740 K is used because this value has been repeatedly measured at the surface from multiple landers (Basilevsky & Head, 2003).

### 2.2.3. Basal Temperature Variations

The higher ambient atmospheric temperature of Venus also results in a warmer ground temperature, which impacts the heat loss to the ground through conduction ( $Q_{\text{cond}}$ ). The conductive heat loss is defined in the PyFLOWGO model (after Keszthelyi, 1995) (Equation 7):

$$Q_{\text{cond}} = K_{\text{lava}} \frac{T_{\text{core}} - T_{\text{base}}}{h_{\text{base}}} w \quad (7)$$

where  $K_{\text{lava}}$  is the thermal conductivity of the lava (W/mK),  $T_{\text{core}}$  is the lava core temperature (K),  $T_{\text{base}}$  is the temperature of the basal layer (K), and  $h_{\text{base}}$  is the thickness of the basal layer (m). For terrestrial studies, it is assumed that the underlying surface temperature is elevated by the overlaying active flow. For example, a basal temperature of 773 K was used for the terrestrial model case (Table 1) (Ramsey et al., 2019). However, to assess the effects of a warmer substrate, its temperature is increased by 100 K increments up to 1173 K. This end member value is below the solidus temperature determined for the terrestrial case (i.e., 1253 K). Anything above the solidus temperature would promote thermal erosion, which has been proposed as a possible mechanism occurring on Venus (Zimbelman et al., 2000). However, it is outside the current capabilities of PyFLOWGO to simulate.

The “Hot-Small-Earth” case using a basal temperature of 773 K produced a channel length of 39.4 km, which increased to 40.3 km at 1173 K. Each increase of 100 K to the basal temperature, therefore, resulted in a slightly lower conductive heat loss and a  $\sim 200$  m increase in channel length (Figure 6). This increase is not significant relative to the other variations produced by the modeled changes thus far. Therefore, a basal temperature of 773 K is used for the remainder of the cases. The limited influence of conductive heat flux is also consistent with that determined for Martian channelized flows (Rowland et al., 2004).

### 2.3. Effects of Atmospheric Heat Capacity and Wind Speed (“Venus-Light”)

Compositional differences between the atmosphere of Earth and Venus affect its specific heat capacity. For terrestrial lava flows, a specific heat capacity of 1,099 J/kg/K is commonly used (e.g., Harris & Rowland, 2001; Harris

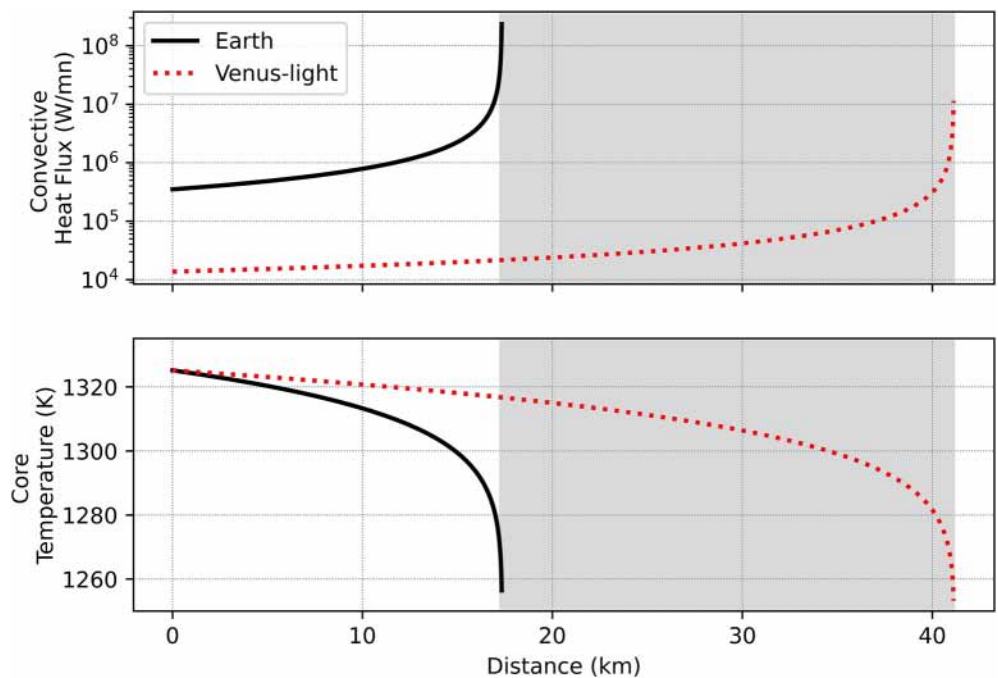


**Figure 7.** Variation in modeled channel length with distance from the vent for convective heat flux and core temperature for the “Earth” and “Venus-light” cases. The gray region indicates the stopping range between the two cases.

et al., 2022; Ramsey et al., 2019). Here, we use 1,181 J/kg/K based on the reported atmospheric composition (Lebonnois et al., 2010). Furthermore, the average wind speed on Venus determined through direct and indirect measurements ranges from 0.3 to 1 m/s (Basilevsky & Head, 2003). We therefore reduce the wind speed from an average of 5 m/s used for Earth modeling to 1 m/s.

The “Venus-light” case produced a lava flow with a channel length of 41.1 km, a 4% increase from the “Hot-Small-Earth” case and an 81% increase from the “Earth” case (Figure 7). This increase in channel length is predominantly due to the decrease in heat loss through forced atmospheric convection. On average, the “Venus-light” case loses  $1.9 \times 10^6$  W/m less heat per unit step of the model through atmospheric convection than the “Earth” case. The lower heat loss from atmospheric convection due to reduced wind speed is consistent with terrestrial observations of lava flows (Keszthelyi et al., 2003).

Thus far, all planetary and environmental changes made to the model for Venus conditions have resulted in an 81% increase in the lava flow channel length.

#### 2.4. Effects of Atmospheric Density (“Venus-Heavy”)

The next change examines the effects of Venusian atmospheric density on the propagation of a channelized lava flow. The atmospheric density of Venus ( $67 \text{ kg/m}^3$ ) is two orders of magnitude greater than that of Earth ( $0.4412 \text{ kg/m}^3$ ) (Lebonnois & Schubert, 2017), resulting in a difference in atmospheric pressure 92 times that of Earth (Read, 2013). Because of this, the modeled channel length for the “Venus-Heavy” case only reached a distance of 15.1 km, which is 92.5% shorter than the “Venus-light” run; and a 13.5% decrease compared to the “Earth” case (Figure 8). Atmospheric density directly affects the heat loss calculated by increasing the efficiency of convection (Equation 4), which results in a higher cooling and crystallization rate and thus, higher viscosity and yield strength (Figure 9). Although the “Venus-Heavy” case does result in more crust cover, it is not sufficient to offset the large convective heat loss.

Basilevsky and Head (2003) reported that the atmospheric density can vary between  $36 \text{ kg/m}^3$  on mountains to  $74 \text{ kg/m}^3$  in deep depressions. To assess the impact on the model from this variability, we performed additional modeling using atmospheric density values every  $5 \text{ kg/m}^3$  between  $35$  and  $75 \text{ kg/m}^3$  (Figure 10). As expected, the results indicate that with decreasing atmospheric density, the forced atmospheric convective heat loss becomes

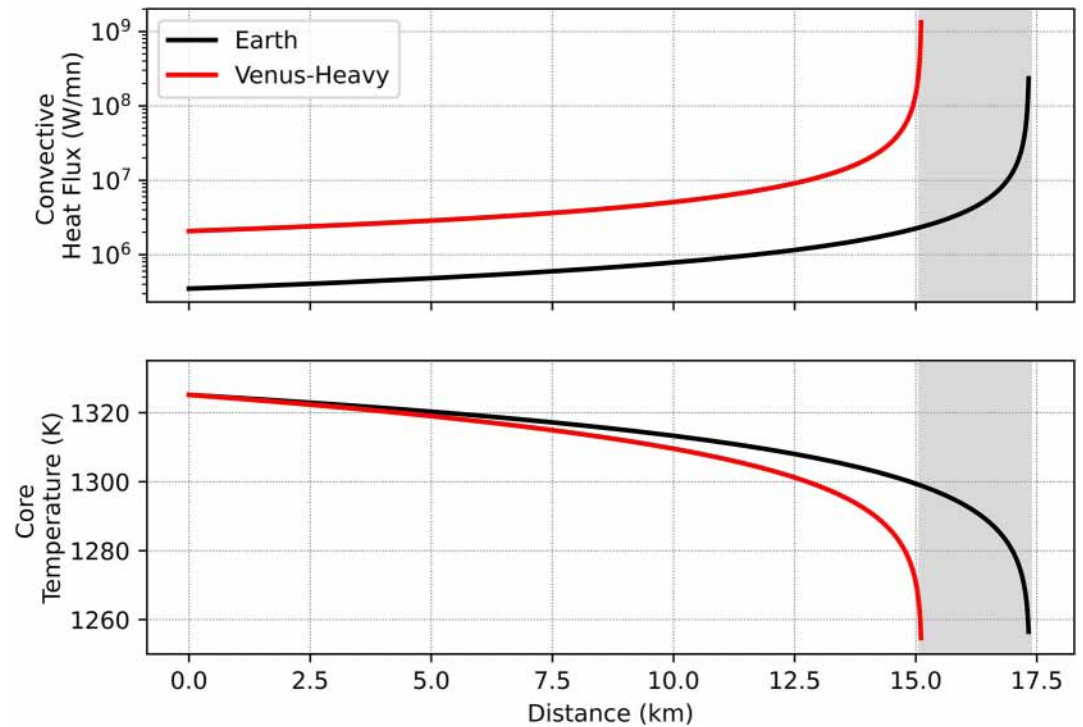


**Figure 8.** Variation in modeled channel length with distance from the vent for convective heat flux and core temperature for the “Earth” and “Venus-Heavy” cases. The gray region indicates the stopping range between the two cases.

less efficient, causing the flow to retain more heat and travel slightly further (Figure 10). At the lowest atmospheric density, the channel length is 21.7 km, whereas at the highest it is 14 km. This is an 8.7 km decrease in length, caused by the  $\sim 1.8 \times 10^6$  W/m increase in convective heat loss per unit step of the model for every  $5 \text{ kg/m}^3$  increase in atmospheric density. In summary, a flow is 43% shorter emplaced in lowest elevations of Venus compared to the highest.

### 2.5. Coupled Convective and Radiative Atmospheric Heat Flux (“Simulated-Venus”)

Snyder (2002) proposed that the dense  $\text{CO}_2$  rich atmosphere of Venus causes coupling of the convective and radiative heat flux, as opposed to the Earth’s atmosphere. The coupling of these two processes results in a reduction of heat flux and the emplacement of a longer lava flow. Using the lava flow surface temperature cooling curve presented in Snyder (2002), we incorporated an approximation of the proposed coupled convective and radiative atmospheric heat flux using Equation 8:

$$Q_{\text{Snyder}} = (1.07 \cdot 10^{-13} T_{\text{surf}}^{4.85} w) * 1000 \quad (8)$$

where  $Q_{\text{Snyder}}$  is the coupled radiative and convective heat flux (W/m). However, instead of a uniform lava surface temperature, as used in Snyder (2002), we use the effective surface temperature ( $T_{\text{surf}}$ ) that accounts for the temperature differences between the crusted ( $T_{\text{crust}}$ ) and un-crusted surface ( $T_{\text{hot}}$ ) of the lava flow (Equation 9).

$$T_{\text{surf}} = T_{\text{crust}} f_{\text{crust}} + T_{\text{hot}} (1 - f_{\text{crust}}) \quad (9)$$

This representation of a modeled lava flow surface is more characteristic of observed lava flow surfaces (Ramsey et al., 2019; Thompson & Ramsey, 2021). Incorporating Equation 8 into PyFLOWGO together with all the inputs from the “Venus-Heavy” case produced a 38.3 km flow (Figure 11). This is a 75.3% increase in flow length compared to “Earth” and an 86.9% increase over the “Venus-Heavy” case. The 23.2 km increase in flow length compared to the “Venus-Heavy” case is due to the average decrease in heat flux of  $\sim 1.4 \times 10^7$  W/m per model step (Figure 11). Although this is only a first-order approximation of the equations from Snyder (2002), this result

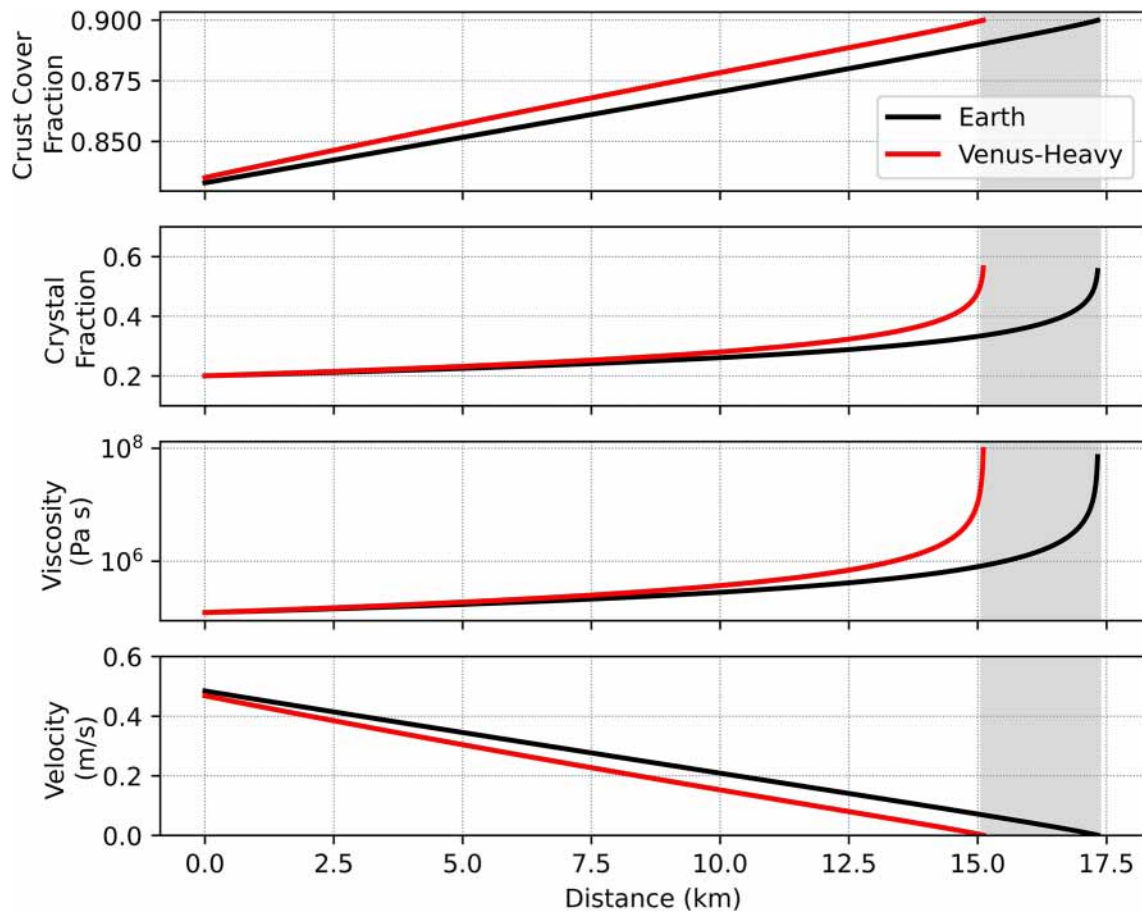


**Figure 9.** Variation in modeled channel length with distance from the vent for the crust cover fraction, crystal fraction, viscosity, and velocity for the “Earth” and “Venus-Heavy” cases (from top to bottom). The gray region indicates the stopping range between the two cases.

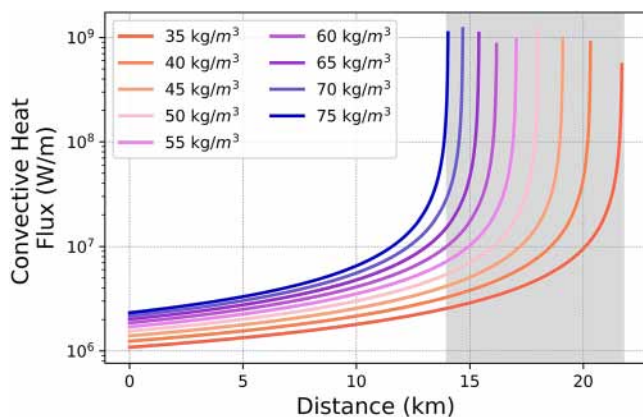


**Figure 10.** Differences in modeled channel length with distance from the vent versus convective heat flux for a range of atmospheric densities observed and expected on the surface of Venus. The gray region indicates the stopping range for all modeled atmospheric densities.

follows his proposed trend and does account for all the environmental variables explored in the prior steps. For the remainder of the work presented, we use the “Simulated-Venus” case.

## 2.6. Effusion Rate

With the model fully adapted to the Venus environment, a final step examines the effusion rates required to reproduce a channelized flow on Venus. This is done by increasing the effusion rate in PyFLOWGO until a desired flow length is matched. Here, we model a 100 km long channelized lava flow with the baseline “Simulated-Venus” rheological and topographic parameters. An effusion rate of  $\sim 1,950 \text{ m}^3/\text{s}$  is required to produce this flow, compared to  $\sim 4,700 \text{ m}^3/\text{s}$  for an equivalent terrestrial flow. Thus, a lower effusion rate on Venus produces the same channel length flow as on Earth. For context, recent large terrestrial eruptions such as the Tolbachik 2012–2013 event produced an  $\sim 16 \text{ km}$  long channelized flow with an initial maximum average effusion rate of  $\sim 440 \text{ m}^3/\text{s}$  (Belousov et al., 2015). Additionally, the 2014–2015 Holuhraun and 2018 Kilauea eruptions produced channelized lava flows,  $\sim 17$  and  $\sim 12 \text{ km}$  long respectively, with instantaneous peak effusion rates of  $\sim 350$ – $\sim 1,700 \text{ m}^3/\text{s}$ , respectively (Patrick et al., 2019; Pedersen et al., 2017).

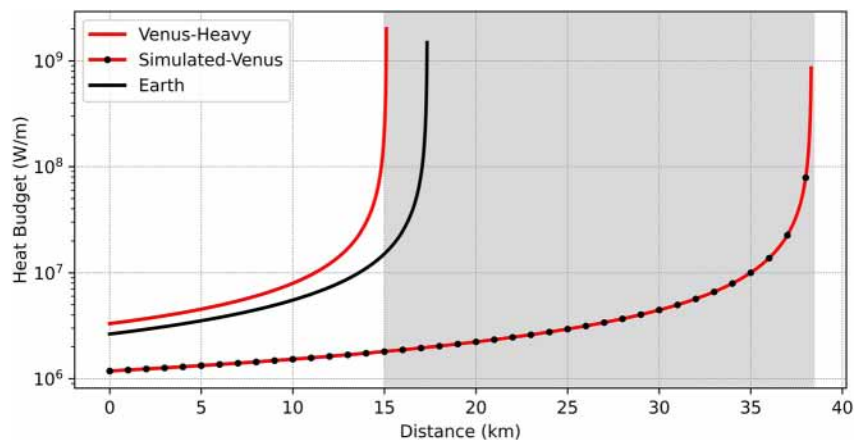


**Figure 11.** Variations in modeled channel length with distance from the vent for the total heat budget for the “Earth,” “Venus-Heavy,” and “Simulated-Venus” cases. The gray region indicates the stopping range between the “Venus-Heavy” case and the “Simulated-Venus” case.

It is important to note that PyFLOWGO accounts for the environmental conditions responsible only for heat loss from the lava flow and not the conditions at the vent that might affect parameters such as the effusion rate. Furthermore, atmospheric pressure is expected to have an impact on the size of volcanic edifices formed, with larger edifices at higher elevations and smaller at lower elevations (Head & Wilson, 1992; Keddie & Head, 1994). Despite the model’s inability to account for the at-vent conditions, we do observe the expected trend with lava flow length and atmospheric density (atmospheric density being correlated with elevation on Venus) (see Section 2.4 and Figure 10).

### 3. Discussion

In this study using the PyFLOWGO model we show that a lava flow having terrestrial characteristics but emplaced on Venus would be substantially longer (up to 81%) for a majority of the planetary and environmental conditions analyzed. We find that the heat loss due to atmospheric convection is higher on Venus than on Earth due to the denser atmosphere, which dominates the flow cooling and produces a shorter (up to 21%) channel length (Figure 12). However, due to the dense CO<sub>2</sub> rich atmosphere and the subsequent coupling of convective and radiative atmospheric heat flux, a Venusian flow should travel (up to 75.3%) further than the Earth equivalent (Figure 12). This modeling result is consistent with observations of the volcanic provinces across the planet that show channelized lava flows appear to be longer than those observed on Earth. We postulate, based on the modeling results here, that the flow length difference is simply due to environmental conditions rather than the need to invoke unusually high effusion rates.

#### 3.1. Previous Modeling Studies

As highlighted in Wilson and Head (1983) Venusian eruptions could have larger effusion rates due to the higher planetary crustal temperature that would limit magma cooling during ascent. Other studies have used flow dimensions to determine effusion rates for Venusian lava flows based on empirical relationships, with values ranging from  $\sim 1 \times 10^3$  to  $1 \times 10^7$  m<sup>3</sup>/s (Gaddis, 1989; Head & Wilson, 1986; Head et al., 1993; Lancaster et al., 1995). For example, Head and Wilson (1986) performed an analysis of open channel flows on Venus, finding that for gradual slopes (<1°), effusion rates greater than  $1 \times 10^4$  m<sup>3</sup>/s are required to emplace flows longer than 100 km. However, our results for a similar slope and flow length scenarios require an effusion rate that is an order of magnitude lower ( $\sim 1,950$  m<sup>3</sup>/s), and more similar to larger eruption rates found on Earth. Our estimated effusion rates are lower than previous studies because PyFLOWGO enables a more refined and adaptable heat budget model (i.e., the effective emissivity model Ramsey et al., 2019; Thompson & Ramsey, 2021; and the coupled radiation-convection model, Snyder, 2002). Additionally, prior studies investigated a range of lava flow morphologies and lengths, which could contribute to the large range in effusion rate values. Certain lava flow

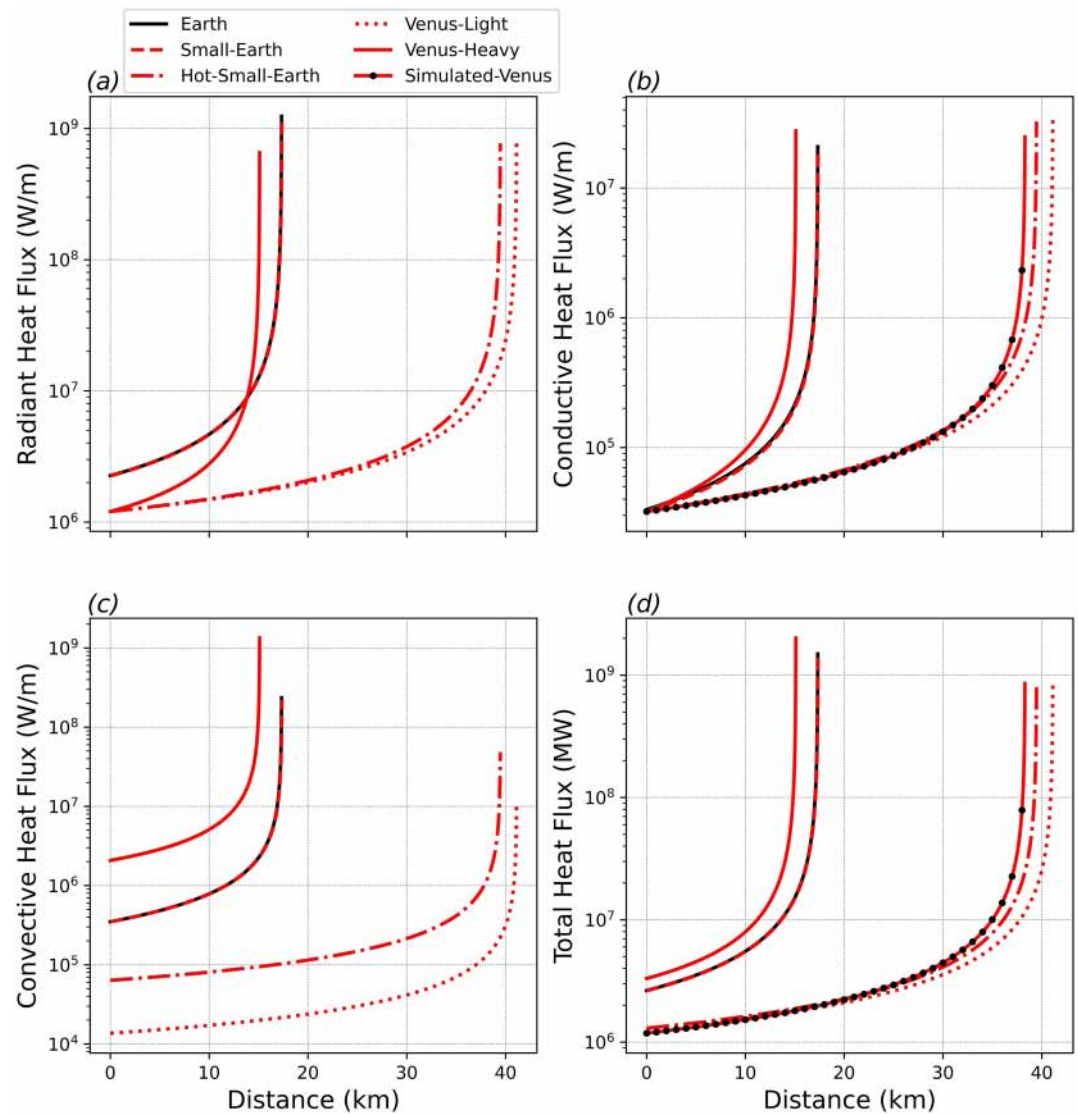


**Figure 12.** Variation in modeled channel length with distance from the vent for the heat loss terms for each of the cases from the “Earth” to “Simulated-Venus”; (a) radiant heat flux, (b) conductive heat flux, (c) convective heat flux, and (d) total heat flux. The “Simulated-Venus” case is not shown on plots (a) and (c) because the radiant and convective heat fluxes are coupled.

morphologies (i.e., sheet flows, lava tubes, channels) and textures (i.e., ‘a’ā and pahoehoe) are related to higher or lower effusion rate values (Gregg, 2017).

High effusion rate eruptions can also produce turbulent flows reflected by larger Reynold's numbers ( $>2,000$ ). Such eruptions may have produced the very longest flows and/or the sinuous rilles/canali seen on Venus (Head et al., 1991; Komatsu et al., 1992; Sakimoto & Gregg, 2001). However, Head and Wilson (1986) investigated several long Venus lava flows (36–2,821 km) that required moderate to high effusion rates for emplacement, and found Reynolds numbers no higher than 75. Using the Reynolds number equation presented in their paper and the viscosity, lava density, and velocity from the “Simulated-Venus” 100 km flow case, we calculated a Reynolds number of 0.15, which clearly indicates that our modeled channelized flows are laminar.

The effects of the Venusian environment on the propagation of channelized, cooling-limited lava flows have also been investigated using a variety of analytical techniques, and analog environments, which produced contradictory

results (Crumpler et al., 2000; Gregg & Greeley, 1993; Head & Wilson, 1986; Hultgrien, 2001; Snyder, 2002). For example, Gregg and Greeley (1993) determined that lava flows, specifically those associated with Venusian canali, have a greater heat loss (due to atmospheric convection and radiation) than an equivalent flow on Earth. However, the flows travel farther due to the development of a thick insulating crust that keeps the lava liquid over a greater distance. These findings are similar to those from Head and Wilson (1986), who identified heat loss by atmospheric convection as the dominant cooling mechanism for open channel lava flows. Specifically, they found that for temperatures above 900 K, the heat loss is about 1.5 times greater than that of an equivalent terrestrial flow. Their study also concluded that lava flows on Venus should cool quicker but ultimately travel farther due to the thicker insulating crust forming early in the flow's emplacement. Our “Venus-Heavy” results agree with those prior studies in that convective heat flux is greater on Venus; however, we propose that this should result in a shorter flow length due to the increased efficiency of convective heat flux, with all other emplacement conditions being equal.

In contrast to those findings, Snyder (2002) determined that convective and radiant heat loss is actually reduced due to the strong infrared CO<sub>2</sub> absorptions (e.g., ~2.7, ~4.2, and ~15.4 μm) combined with the dense atmosphere. This reduction in heat loss causes the flows to cool 30%–40% slower, thus producing longer flows (Snyder, 2002). We incorporate an approximation of the proposed coupled convective and radiative atmospheric heat flux in PyFLOWGO, the “Simulated-Venus” case. This resulted in a longer lava flow than the equivalent terrestrial case, consistent with the results predicted in Snyder (2002), and observations of channelized lava flows on the Venusian surface.

Importantly, the original work of Snyder (2002) assumed that the lava flow's surface has a uniform emissivity of 1.0. This is inaccurate and can have quantifiable impacts on the derived radiative heat flux (i.e., Ramsey et al., 2019; Thompson & Ramsey, 2021). Although the Snyder's (2002) approximation is an improvement to the PyFLOWGO model and provides results that are consistent with observations of Venusian lava flows, additional detailed laboratory studies of lava emission in a CO<sub>2</sub>-rich environment are needed to fully validate the results.

Our results for the first three adaptation steps initially followed the same trend predicted by prior studies, which showed that environmental conditions on Venus should promote an increased channel length compared to an equivalent terrestrial lava flow. However, in the “Venus-Heavy” case, our results indicate that the atmospheric density significantly increases the efficiency of convective heat loss, resulting in shorter modeled channel lengths. This result is similar to the conclusions of Head and Wilson (1986) and Gregg and Greeley (1993), who conclude that convective heat loss is a critical factor in the emplacement of a Venusian lava flow; however, they invoke a thicker, insulating crust and long-duration, high-volume eruptions to produce the longer flows. However, neither of these studies considered the effects of the coupled convective and radiative heat flux. Here we show that this results in a longer lava flow (~75%) than the Earth equivalent. A lower effusion rate can indeed produce the longer channelized flows seen on Venus without the need to invoke a thicker insulating crust. However, PyFLOWGO is not currently able to replicate increasing crust thickness downflow nor a flow that becomes fully confined to a tube, neither of which are expected at clearly defined open channelized flows. Rather, a crust cover fraction (of a unconstrained thickness) in the model relates to the surface radiative and convective heat flux equations (Equations 2 and 5). Thus, an increase in crust cover results in reduced radiative and convective heat flux, but never to the point of affecting the conductive heat loss from the top of the flow or producing a lava tube. Our results do show that the open channelized lava flows on Venus should have a higher crust cover fraction compared to the equivalent terrestrial flow (Figure 9).

A prior study applied an older version of the FLOWGO model to Venusian canali (Harrington & Williams-Jones, 2017). However, the emplacement mechanisms for canali are theorized to be different from those of channelized lava flows (i.e., require thermal and/or mechanical erosion), or require exotic compositions (Gregg & Greeley, 1993; Komatsu et al., 1992). Therefore, FLOWGO may not be appropriate to reproduce the emplacement of the canali features, barring changes to the internal workings and assumptions of the model. Using the model to investigate Venusian channelized lava flows is appropriate, however, and assumes that the processes that form the channels are similar or the same to those on Earth. For example, the observations of Venusian channelized flows indicate that the surface texture is similar to terrestrial ‘a’ā flows (Campbell & Campbell, 1992), potentially indicating similar channel formation mechanisms.

### 3.2. Emplacement Time and Volume Estimates

An objective for the upcoming orbital Venus missions (i.e., VERITAS and EnVision) is to search for very recent or newly active volcanic activity (Helbert et al., 2019; Smrekar et al., 2022). Important considerations in the search for new volcanic activity are the volume and emplacement time of the lava flows. In other words, would a new channelized flow be large enough or stay hot long enough for its thermal emission to be detected with the near infrared instruments?

Using PyFLOWGO we can only estimate the time for the lava to travel in the channel from the vent to the flow front based on the calculated velocity and the maximum flow length (Harris & Rowland, 2001). The initial “Earth” model case would travel at an average velocity of 0.24 m/s and hence reach the flow front (17.3 km) in 55 hr. In the “Simulated-Venus” case, the lava would travel at an average velocity of 0.23 m/s in the channel and reach the flow front (38.3 km) in 126 hr. For a 100 km-long simulated Venusian lava flow, it would take 179 hr. By comparison, large terrestrial channelized lava flows (e.g., those from the 2018 Kilauea eruption) have channel velocity of the order of 5–15 m/s (Dietterich et al., 2021).

Using the modeled channel widths and lengths produced from PyFLOWGO for the 38.3 and 100 km “Simulated-Venus” flows, the surface area for each channel would be 15.5 and 42.8 km<sup>2</sup>, respectively. Incorporating the channel depth measurement used in the model (8.7 m), the volume for the two flows would be 0.13 and 0.37 km<sup>3</sup>, respectively. Both of these simulated flows would therefore be large enough to be observed with the proposed spatial resolution of the Venus Interferometric Synthetic Aperture Radar (VISAR) and Venus Emissivity Mapper (VEM) instruments on the upcoming VERITAS mission, for example, (Smrekar et al., 2022). An important caveat is that PyFLOWGO does not account for the levee development or growth during the flow's emplacement, and therefore the calculated surface area represents a minimum estimate (e.g., only the channel). Additionally, the channel depth is held constant throughout the model run, which is consistent with many terrestrial flows (Lipman & Banks, 1987). However, any variation in channel depth would affect the calculated flow volume.

Combining the calculated volumes for the simulated lava flows and the modeled effusion rates, we can determine emplacement times as well. Using the volumes for the “Simulated-Venus” flows of 38.3 and 100 km in length, and an effusion rate of 1,950 m<sup>3</sup>/s, the emplacement times would be 19 and 53 hr, respectively. The calculated emplacement times presented here are for a single channelized lava flow and do not account for any volcanic precursory activity, multiple flow emplacements, or the residual radiant energy released from cooling flows (or other volcanic products) after an eruption has ceased. These emplacement times should be treated as minimum estimates but provide a baseline for upcoming mission observations. In theory, based on the orbital period (6.1-hr for phase I and 91-min for phase II) of the VERITAS mission and the calculated emplacement times presented here, an actively cooling flow would be detected by the VISAR and VEM instruments (Smrekar et al., 2022).

## 4. Conclusion

We adapted the terrestrial PyFLOWGO model to Venusian environmental and planetary conditions to assess how each change affects the dynamics of a channelized lava flow emplacement. PyFLOWGO is the preferred model of choice because it accounts for rheologic and thermal changes, is highly adaptable with different modules available, and is easily modified for other planetary conditions. Our modeling was accomplished in five steps by changing the following conditions: (a) gravity (i.e., “Small-Earth”), (b) ambient atmospheric temperature (i.e., “Hot-Small-Earth”), (c) atmospheric specific heat capacity and wind speed (i.e., “Venus-light”), (d) atmospheric density (i.e., “Venus-Heavy”), (e) and coupling atmospheric convective and radiative heat flux (i.e., “Simulated-Venus”). The coupling of atmospheric convective and radiative heat flux causes significant change between a Venusian channelized flow and its terrestrial equivalent. This resulted in a significant reduction in overall heat flux and subsequently increased the flow length by ~75%.

Because lava flow length is positively correlated with effusion rate for most conditions, only moderately higher effusion rates than those for typical terrestrial eruption are required to model the equivalent lava flows on Venus. However, given the modeled rheologic properties of the studied lava flow and assumed environmental conditions, the effusion rate determined here (1,950 m<sup>3</sup>/s) is at the very low-end range of past studies that used other models ( $\sim 1 \times 10^3$ – $1 \times 10^7$  m<sup>3</sup>/s) (Gaddis, 1989; Head & Wilson, 1986; Head et al., 1993; Lancaster et al., 1995).



Alternatively, emplacement processes currently outside the ability of PyFLOWGO to reproduce could be a factor in modeling Venusian lava flows (i.e., a thicker insulating crust and/or thermal erosion). Future work will focus on developing improvements and adaptations to PyFLOWGO, including (a) laboratory validation of lava heat flux in a CO<sub>2</sub> environment (Snyder, 2002), and (b) implementing variations in crust thickness in an open channel as the flow advances.

With the three planned missions to Venus (i.e., DAVINCI+, VERITAS, and EnVision) in the next decade, new surface emissivity data, improved atmospheric knowledge, higher resolution radar surface images, and topography will become available. Specifically, one of the key science objectives of the VERITAS mission is to assess volcanic activity across the surface of Venus (Smrekar et al., 2022). This will be accomplished using the VEM instrument to search for elevated thermal emission associated with active volcanism, and the VISAR instrument to detect topographic changes caused by recent/active flows. Synergistic surface observations from the VERITAS and EnVision missions will also aid in the search of active volcanism. Therefore, understanding the rate at which new lava flows may be emplaced and cool is important for mission planning, science requirements, and data observations.

### Data Availability Statement

The PyFLOWGO model is available for download at <https://github.com/pyflowgo>. All PyFLOWGO data discussed in this paper are available to the public (Flynn, 2022).

### Acknowledgments

This research was supported through the NASA Solar System Workings (SSW) program (Grant 80NSSC19K0547). The authors would like to thank Scott Rowland, Steve Baloga, and an anonymous reviewer for their insightful reviews. The authors would also like to thank Tracy Gregg and David Crown for their constructive discussions relating to Venus's volcanism. This is Laboratory of Excellence ClerVolc contribution no. 576.

### References

- Ashley, K. T., & Ramsey, M. S. (2019). Equilibrium crystallization modeling of Venusian lava flows incorporating data with large geochemical uncertainties. *Earth and Planetary Science Letters*, 516, 156–163. <https://doi.org/10.1016/j.epsl.2019.03.036>
- Baloga, S. M., & Glaze, L. S. (2008). A self-replication model for long channelized lava flows on the Mars plains. *Journal of Geophysical Research E: Planets*, 113(5), 1–15. <https://doi.org/10.1029/2007JE002954>
- Basilevsky, A. T., & Head, J. W. (2003). The surface of Venus. *Reports on Progress in Physics*, 66(10), 1699–1734. <https://doi.org/10.1088/0034-4885/66/10/R04>
- Belousov, A., Belousova, M., Edwards, B., Volynets, A., & Melnikov, D. (2015). Overview of the precursors and dynamics of the 2012–13 basaltic fissure eruption of Tolbachik Volcano, Kamchatka, Russia. *Journal of Volcanology and Geothermal Research*, 307, 22–37. <https://doi.org/10.1016/j.jvolgeores.2015.06.013>
- Byrne, P. K., & Krishnamoorthy, S. (2021). Estimates on the frequency of volcanic eruptions on Venus. *Journal of Geophysical Research: Planets*, 127, 1–16. <https://doi.org/10.1029/2021je007040>
- Byrnes, J. M., & Crown, D. A. (2002). Morphology, stratigraphy, and surface roughness properties of Venusian lava flow fields. *Journal of Geophysical Research E: Planets*, 107(10), 5079. <https://doi.org/10.1029/2001je001828>
- Campbell, B. A., & Campbell, D. B. (1992). Analysis of volcanic surface morphology on Venus from comparison of Arecibo, Magellan, and terrestrial airborne radar data. *Journal of Geophysical Research*, 97(E10), 16293–16314. <https://doi.org/10.1029/92je01558>
- Chevrel, M. O., Labroquere, J., Harris, A. J. L., & Rowland, S. K. (2018). PyFLOWGO: An open-source platform for simulation of channelized lava thermo-rheological properties. *Computers & Geosciences*, 111, 167–180. <https://doi.org/10.1016/j.cageo.2017.11.009>
- Churikova, T. G., Gordeychik, B. N., Edwards, B. R., Ponomareva, V. V., & Zelenin, E. A. (2015). The Tolbachik volcanic massif: A review of the petrology, volcanology and eruption history prior to the 2012–2013 eruption. *Journal of Volcanology and Geothermal Research*, 307, 3–21. <https://doi.org/10.1016/j.jvolgeores.2015.10.016>
- Crisp, J., & Baloga, S. (1990). A model for lava flows with two thermal components. *Journal of Geophysical Research*, 95(B2), 1255–1270. <https://doi.org/10.1029/jb095ib02p01255>
- Crumpler, L. S., Gregg, T. K. P., Sakimoto, S. E. H., & Sakimoto, S. (2000). Volcanism on Earth's seafloor and Venus. *Environmental Effects on Volcanic Eruptions*, 113–142. <https://doi.org/10.1007/978-1-4615-4151-6>
- Daneš, Z. F. (1972). Dynamics of lava flows. *Journal of Geophysical Research*, 77(8), 1430–1432. <https://doi.org/10.1029/jb077i008p01430>
- Dieterich, H. R., Diefenbach, A. K., Soule, S. A., Zoeller, M. H., Patrick, M. P., Major, J. J., & Lundgren, P. R. (2021). Lava effusion rate evolution and erupted volume during the 2018 Kilauea lower East Rift Zone eruption. *Bulletin of Volcanology*, 83(4), 25. <https://doi.org/10.1007/s00445-021-01443-6>
- D'Incecco, P., Filiberto, J., Lopez, I., Gorinov, D., & Komatsu, G. (2021). Idunn Mons: Evidence for ongoing volcano-tectonic activity and atmospheric implications on Venus. *Journal of Geophysical Research*, 2(5), 215. <https://doi.org/10.3847/PSJ/ac2258>
- D'Incecco, P., Müller, N., Helbert, J., & D'Amore, M. (2017). Idunn Mons on Venus: Location and extent of recently active lava flows. *Planetary and Space Science*, 136, 25–33. <https://doi.org/10.1016/j.pss.2016.12.002>
- Fedotov, S. A., Balessta, S. T., Dvigalo, V. N., Razina, A. A., Flerov, G. B., & Chirkov, A. M. (1991). New Tolbachik volcanoes. *Active Volcanoes of Kamchatka*, 1, 214–281.
- Filiberto, J. (2014). Magmatic diversity on Venus: Constraints from terrestrial analog crystallization experiments. *Icarus*, 231, 131–136. <https://doi.org/10.1016/j.icarus.2013.12.003>
- Filiberto, J., Trang, D., Treiman, A. H., & Gilmore, M. S. (2020). Present-day volcanism on Venus as evidenced from weathering rates of olivine. *Science Advances*, 6(1), 2–6. <https://doi.org/10.1126/sciadv.aax7445>
- Flynn, I. T. W. (2022). PyFLOWGO goes to Venus. <https://doi.org/10.5281/ZENODO.7415730>
- Flynn, I. T. W., Crown, D. A., & Ramsey, M. S. (2021). The effects of DEM resolution on planetary thermo-rheological lava flow modeling. In *52nd lunar and planetary science conference* (p. 1305).
- Flynn, I. T. W., Crown, D. A., & Ramsey, M. S. (2022). Determining emplacement conditions and vent locations for channelized lava flows southwest of Arsia Mons. *Journal of Geophysical Research: Planets*, 127(11), e2022JE007467. <https://doi.org/10.1029/2022JE007467>

- Ford, P. G., & Pettengill, G. H. (1992). Venus topography and kilometer-scale slopes. *Journal of Geophysical Research*, 97(E8), 103–114. <https://doi.org/10.1029/92je01085>
- Gaddis, L. R. (1989). Estimates of minimum lava flow eruption rates on Venus. In *Lunar and planetary science conference* (Vol. 20).
- Giordano, D., Russell, J. K., & Dingwell, D. B. (2008). Viscosity of magmatic liquids: A model. *Earth and Planetary Science Letters*, 271(1–4), 123–134. <https://doi.org/10.1016/j.epsl.2008.03.038>
- Greeley, R., & Iversen, J. D. (1987). Measurements of wind friction speeds over lava surfaces and assessment of sediment transport. *Geophysical Research Letters*, 14(9), 925–928. <https://doi.org/10.1029/gi014i009p00925>
- Gregg, T. K. P. (2017). Patterns and processes: Subaerial lava flow morphologies: A review. *Journal of Volcanology and Geothermal Research*, 342, 3–12. <https://doi.org/10.1016/j.jvolgeores.2017.04.022>
- Gregg, T. K. P., & Greeley, R. (1993). Formation of Venusian canali: Considerations of lava types and their thermal behaviors. *Journal of Geophysical Research*, 98(E6), 873–882. <https://doi.org/10.1029/93je00692>
- Gregg, T. K. P., & Sakimoto, S. E. H. (1996). Venusian lava flow morphologies: Variations on a basaltic theme. In *Lunar and planetary science conference* (Vol. 27).
- Harrington, E., & Williams-Jones, G. (2017). Preliminary thermorheological modeling of silicate melts in Venusian Canali. In *48th lunar and planetary science conference*. Lunar and Planetary Institute.
- Harris, A. J., & Rowland, S. (2001). FLOWGO: A kinematic thermo-rheological model for lava flowing in a channel. *Bulletin of Volcanology*, 63(1), 20–44. <https://doi.org/10.1007/s004450000120>
- Harris, A. J. L., Rowland, S. K., & Chevrel, M. O. (2022). The anatomy of a channel-fed ‘a’a lava flow system. *Bulletin of Volcanology*, 84, 70. <https://doi.org/10.1007/s00445-022-01578-0>
- Head, J. W., Campbell, D. B., Elachi, C., Guest, J. E., McKenzie, D. P., Saunders, R. S., et al. (1991). Venus volcanism: Initial analysis from Magellan data. *Science*, 252(5003), 276–288. <https://doi.org/10.1126/science.252.5003.276>
- Head, J. W., Crumpler, L. S., Aubele, J. C., & Saunders, R. S. (1992). Venus volcanism: Classification of volcanic features and structures, associations, and global distribution from Magellan data. *Journal of Geophysical Research*, 97(9), 13153. <https://doi.org/10.1029/92je01273>
- Head, J. W., Roberts, K. M., Wilson, L., & Pinkerton, H. (1993). Lava flow-field morphological classification and interpretation: Examples from Venus. In *Lunar and planetary science conference* (Vol. 24).
- Head, J. W., & Wilson, L. (1986). Volcanic processes and landforms on Venus: Theory, predictions, and observations. *Journal of Geophysical Research*, 91(B9), 9407. <https://doi.org/10.1029/jb091ib09p09407>
- Head, J. W., & Wilson, L. (1992). Magma reservoirs and neutral buoyancy zones on Venus: Implications for the formation and evolution of volcanic landforms. *Journal of Geophysical Research*, 97(E3), 3877–3903. <https://doi.org/10.1029/92je00053>
- Helbert, J., Vandaele, A. C., Marcq, E., Robert, S., Ryan, C., Guignan, G., et al. (2019). The VenSpec suite on the ESA EnVision mission to Venus. In *Infrared remote sensing and instrumentation XXVII* (Vol. 11128, pp. 18–32). SPIE.
- Herrick, R. R., & Hensley, S. (2023). Surface changes observed on a Venusian volcano during the Magellan mission. *Science*, 379(6638), 1205–1208. <https://doi.org/10.1126/science.abm7735>
- Herrick, R. R., Stahlke, D. L., & Sharpton, V. L. (2012). Fine-scale Venusian topography from Magellan stereo data. *Eos*, 93(12), 125–126. <https://doi.org/10.1029/2012EO120002>
- Hiesinger, H., Head, J., & Neukum, G. (2007). Young lava flows on the eastern flank of Ascraeus Mons: Rheological properties derived from High Resolution Stereo Camera (HRSC) images and Mars Orbiter Laser Altimeter (MOLA) data. *Journal of Geophysical Research E: Planets*, 112(5), E05011. <https://doi.org/10.1029/2006JE002717>
- Hulme, G. (1974). The interpretation of lava flow morphology. *Geophysical Journal of the Royal Astronomical Society*, 39(2), 361–383. <https://doi.org/10.1111/j.1365-246X.1974.tb05460.x>
- Hulme, G. (1976). The determination of the rheological properties and effusion rate of an Olympus Mons lava. *Icarus*, 27(2), 207–213. [https://doi.org/10.1016/0019-1035\(76\)90004-X](https://doi.org/10.1016/0019-1035(76)90004-X)
- Hultgrien, L. K. (2001). *The cooling of terrestrial basaltic lava flows and implications for lava flow emplacement on Venus from surface morphology and radar data*. Dissertation. John Hopkins University.
- Ivanov, M. A., & Head, J. W. (2013). The history of volcanism on Venus. *Planetary and Space Science*, 84, 66–92. <https://doi.org/10.1016/j.pss.2013.04.018>
- Keddie, S. T., & Head, J. W. (1994). Height and altitude distribution of large volcanoes on Venus. *Planetary and Space Science*, 42(6), 455–462. [https://doi.org/10.1016/0032-0633\(94\)90088-4](https://doi.org/10.1016/0032-0633(94)90088-4)
- Keszthelyi, L. (1995). Measurements of the cooling at the base of pahoehoe flows. *Geophysical Research Letters*, 22(16), 2195–2198. <https://doi.org/10.1029/95GL01812>
- Keszthelyi, L., Harris, A. J. L., & Dehn, J. (2003). Observations of the effect of wind on the cooling of active lava flows. *Geophysical Research Letters*, 30(19), 1–4. <https://doi.org/10.1029/2003GL017994>
- Komatsu, G., Kargel, J. S., & Baker, V. R. (1992). Canali-type channels on Venus: Some genetic constraints. *Geophysical Research Letters*, 19(13), 1415–1418. <https://doi.org/10.1029/92gl010147>
- Lancaster, M. G., Guest, J. E., & Magee, K. P. (1995). Great lava flow fields on Venus. *Icarus*, 118(1), 69–86. <https://doi.org/10.1006/icar.1995.1178>
- Lebonnois, S., Hourdin, F., Eymet, V., Crespin, A., Fournier, R., & Forget, F. (2010). Superrotation of Venus’ atmosphere analyzed with a full general circulation model. *Journal of Geophysical Research*, 115(6), 1–23. <https://doi.org/10.1029/2009JE003458>
- Lebonnois, S., & Schubert, G. (2017). The deep atmosphere of Venus and the possible role of density-driven separation of CO<sub>2</sub> and N<sub>2</sub>. *Nature Geoscience*, 10(7), 473–477. <https://doi.org/10.1038/ngeo2971>
- Lee, R. J., & Ramsey, M. S. (2016). What is the emissivity of active basaltic lava flows. In *Proceedings of the AGU fall meeting, San Francisco, CA, USA* (pp. 12–16).
- Lipman, P. W., & Banks, N. (1987). A’ a flow dynamics, 1984 Mauna Loa eruption. *Volcanism in Hawaii*. 43.
- MacLellan, L., Ernst, R., El Bilali, H., Ghail, R., & Bethell, E. (2021). Volcanic history of the Decreto large igneous province, Astkhik Planum, Venus. *Earth-Science Reviews*, 220, 103619. <https://doi.org/10.1016/j.earscirev.2021.103619>
- Mouginis-Mark, P. J. (2016). Geomorphology and volcanology of Maat Mons, Venus. *Icarus*, 277, 433–441. <https://doi.org/10.1016/j.icarus.2016.05.022>
- Mueller, N. T., Smrekar, S., Helbert, J., Stofan, E., Piccioni, G., & Drossart, P. (2017). Search for active lava flows with VIRTIS on Venus Express. *Journal of Geophysical Research: Planets*, 122(5), 1021–1045. <https://doi.org/10.1002/2016JE005211>
- Nikolaeva, O. V., & Ariskin, A. A. (1999). Geochemical constraints on petrogenetic processes on Venus. *Journal of Geophysical Research E: Planets*, 104(E8), 18889–18897. <https://doi.org/10.1029/1996JE000337>

- Patrick, M. R., Dieterich, H. R., Lyons, J. J., Diefenbach, A. K., Parcheta, C., Anderson, K. R., et al. (2019). Cyclic lava effusion during the 2018 eruption of Kīlauea Volcano. *Science*, *366*(6470). <https://doi.org/10.1126/science.aay9070>
- Pedersen, G. B. M., Höskuldsson, A., Dürig, T., Thordarson, T., Jónsdóttir, I., Riisshuus, M. S., et al. (2017). Lava field evolution and emplacement dynamics of the 2014–2015 basaltic fissure eruption at Holuhraun, Iceland. *Journal of Volcanology and Geothermal Research*, *340*, 155–169. <https://doi.org/10.1016/j.jvolgeores.2017.02.027>
- Peters, S. I., Christensen, P. R., & Clarke, A. B. (2021). Lava flow eruption conditions in the Tharsis volcanic province on Mars. *Journal of Geophysical Research: Planets*, *126*(7), e2020JE006791. <https://doi.org/10.1029/2020JE006791>
- Pieri, D. C., & Baloga, S. M. (1986). Eruption rate, area, and length relationships for some Hawaiian lava flows. *Journal of Volcanology and Geothermal Research*, *30*(1–2), 29–45. [https://doi.org/10.1016/0377-0273\(86\)90066-1](https://doi.org/10.1016/0377-0273(86)90066-1)
- Pieri, D. C., Glaze, L. S., & Abrams, M. J. (1990). Thermal radiance observations of an active lava flow during the June 1984 eruption of Mount Etna. *Geology*, *18*(10), 1018–1022. [https://doi.org/10.1130/0091-7613\(1990\)018<1018:TROOAA>2.3.CO;2](https://doi.org/10.1130/0091-7613(1990)018<1018:TROOAA>2.3.CO;2)
- Pinkerton, H., & Wilson, L. (1994). Factors controlling the lengths of channel-fed lava flows. *Bulletin of Volcanology*, *56*(2), 108–120. <https://doi.org/10.1007/BF00304106>
- Pollack, J. B., Toon, O. B., & Boese, R. (1980). Greenhouse models of Venus' High surface temperature, as constrained by Pioneer Venus measurements. *Journal of Geophysical Research*, *85*(A13), 8223. <https://doi.org/10.1029/ja085ia13p08223>
- Ramsey, M. S., Chevrel, M. O., Coppola, D., & Harris, A. J. L. (2019). The influence of emissivity on the thermo-rheological modeling of the channelized lava flows at Tolbachik volcano. *Annals of Geophysics*, *62*(2). <https://doi.org/10.4401/ag-8077>
- Read, P. L. (2013). The dynamics and circulation of Venus atmosphere. In L. Bengtsson, R.-M. Bonnet, D. Grinspoon, S. Koumoutsaris, S. Lebonnois, & D. Titov (Eds.), *Towards understanding the climate of Venus: Applications of terrestrial models to our sister planet* (pp. 73–110). Springer New York. [https://doi.org/10.1007/978-1-4614-5064-1\\_6](https://doi.org/10.1007/978-1-4614-5064-1_6)
- Rhéty, M., Harris, A., Villeneuve, N., Gurioli, L., Médard, E., Chevrel, O., & Bachélery, P. (2017). A comparison of cooling-limited and volume-limited flow systems: Examples from channels in the Piton de la Fournaise April 2007 lava-flow field. *Geochemistry, Geophysics, Geosystems*, *18*(9), 3270–3291. <https://doi.org/10.1002/2017GC006839>
- Roberts, K. M., Guest, E., Head, W., & Lancaster, L. G. (1992). Mylitta Fluctus, Venus: Rift-related, centralized volcanism and the emplacement of large-volume flow units. *Journal of Geophysical Research*, *97*(92), 15991. <https://doi.org/10.1029/92je01245>
- Rowland, S. K., Garbeil, H., & Harris, A. J. L. (2005). Lengths and hazards from channel-fed lava flows on Mauna Loa, Hawai'i, determined from thermal and downslope modeling with FLOWGO. *Bulletin of Volcanology*, *67*(7), 634–647. <https://doi.org/10.1007/s00445-004-0399-x>
- Rowland, S. K., Harris, A. J. L., & Garbeil, H. (2004). Effects of Martian conditions on numerically modeled, cooling-limited, channelized lava flows. *Journal of Geophysical Research E: Planets*, *109*(10), 1–16. <https://doi.org/10.1029/2004JE002288>
- Rowland, S. K., Harris, A. J. L., & Kallianpur, K. (2002). Vent locations on Elysium Mons, Mars, from thermal modeling of lava flows. *LPSC*, *33*(1441), 1–2.
- Ryerson, F. J., Weed, H. C., & Piwinski, A. J. (1988). Rheology of subliquidus magmas: 1. Picritic compositions. *Journal of Geophysical Research*, *93*(B4), 3421–3436. <https://doi.org/10.1029/jb093ib04p03421>
- Sakimoto, S. E. H., & Gregg, T. K. P. (2001). Channeled flow: Analytic solutions, laboratory experiments, and applications to lava flows. *Journal of Geophysical Research*, *106*(B5), 8629–8644. <https://doi.org/10.1029/2000jb900384>
- Saunders, R. S., Spear, A. J., Allin, P. C., Austin, R. S., Berman, A. L., Chandler, R. C., et al. (1992). Magellan mission summary. *Journal of Geophysical Research*, *97*(E8), 13067–13090. <https://doi.org/10.1029/92je01397>
- Smrekar, S., Hensley, S., Nybakken, R., Wallace, M. S., Perkovic-Martin, D., You, T. H., et al. (2022). VERITAS (Venus emissivity, radio science, InSAR, topography, and spectroscopy): A discovery mission. In *IEEE aerospace conference proceedings*. IEEE Computer Society. <https://doi.org/10.1109/AERO53065.2022.9843269>
- Smrekar, S. E., Stofan, E. R., Mueller, N., Treiman, A., Elkins-Tanton, L., Helbert, J., et al. (2010). Recent hotspot volcanism on Venus from VIRTIS emissivity data. *Science*, *328*(5978), 605–608. <https://doi.org/10.1126/science.1186785>
- Snyder, D. (2002). Cooling of lava flows on Venus: The coupling of radiative and convective heat transfer. *Journal of Geophysical Research E: Planets*, *107*(10), 1–8. <https://doi.org/10.1029/2001je001501>
- Thompson, J. O., & Ramsey, M. S. (2021). The influence of variable emissivity on lava flow propagation modeling. *Bulletin of Volcanology*, *83*(6), 1–19. <https://doi.org/10.1007/s00445-021-01462-3>
- Vaucher, J., Baratoux, D., Toplis, M. J., Pinet, P., Mangold, N., & Kurita, K. (2009). The morphologies of volcanic landforms at Central Elysium Planitia: Evidence for recent and fluid lavas on Mars. *Icarus*, *200*(1), 39–51. <https://doi.org/10.1016/j.icarus.2008.11.005>
- Volynets, A. O., Edwards, B. R., Melnikov, D., Yakushev, A., & Griboedova, I. (2015). Monitoring of the volcanic rock compositions during the 2012–2013 fissure eruption at Tolbachik volcano, Kamchatka. *Journal of Volcanology and Geothermal Research*, *307*, 120–132. <https://doi.org/10.1016/j.jvolgeores.2015.07.014>
- Wantim, M. N., Kervyn, M., Ernst, G. G. J., del Marmol, M. A., Suh, C. E., & Jacobs, P. (2013). Numerical experiments on the dynamics of channelized lava flows at Mount Cameroon volcano with the FLOWGO thermo-rheological model. *Journal of Volcanology and Geothermal Research*, *253*, 35–53. <https://doi.org/10.1016/j.jvolgeores.2012.12.003>
- Wilson, L., & Head, J. W., III. (1983). A comparison of volcanic eruption processes on Earth, Moon, Mars, Io and Venus. *Nature*, *302*(5910), 663–669. <https://doi.org/10.1038/302663a0>
- Wilson, L., & Parfitt, E. A. (1993). The formation of perched lava ponds on basaltic volcanoes: The influence of flow geometry on cooling-limited lava flow lengths. *Journal of Volcanology and Geothermal Research*, *56*(1–2), 113–123. [https://doi.org/10.1016/0377-0273\(93\)90053-t](https://doi.org/10.1016/0377-0273(93)90053-t)
- Wright, R., Garbeil, H., & Harris, A. J. L. (2008). Using infrared satellite data to drive a thermo-rheological/stochastic lava flow emplacement model: A method for near-real-time volcanic hazard assessment. *Geophysical Research Letters*, *35*(19), L19307. <https://doi.org/10.1029/2008GL035228>
- Wroblewski, F. B., Treiman, A. H., Bhiravarasu, S., & Gregg, T. K. P. (2019). Ovda Fluctus, the festoon lava flow on Ovda Regio, Venus: Not silica-rich. *Journal of Geophysical Research: Planets*, *124*(8), 2233–2245. <https://doi.org/10.1029/2019JE006039>
- Zimbelman, J. R., Gregg, T. K. P., & Gregg, T. K. P. (2000). *Environmental effects on volcanic eruptions: From deep oceans to deep space*. Springer Science & Business Media.